International Journal on Interactive Design and Manufacturing (IJIDeM)
https://doi.org/10.1007/s12008-022-00865-6

ORIGINAL PAPER

Assessment of close-range photogrammetry for the low cost development of 3D models of car bodywork components

Andrea Petruccioli[1] · **Francesco Gherardini**[1] · **Francesco Leali**[1]

Received: 23 January 2021 / Accepted: 17 February 2022

Abstract
Close-range photogrammetry (C-RP) is a widespread and efficient technology to obtain digital models of physical objects. Typical limitations as sharped geometry, shiny surface finishing and light conditions can be overcome by using high-end equipment, which results in increased costs and requires specific skills in human operators. This paper aims to investigate whether a low-cost and simplified approach to C-RP makes it suitable for the 3D acquisition of bodywork components and similar free-form artefacts, as an affordable alternative to 3D scanning in fields where a lower value of accuracy is required. Hence, two commercial C-RP software were used to 3D capture handcrafted car body panels and compare the C-RP models using a 3D scan as a reference within an inspection software. Two case studies are considered: a 1:5 scale model of the front bonnet of a Ferrari 250 Testa Rossa from 1958 and a head lamp housing of a Ferrari 275 GTB from 1962. Considering the complexity of double curvature surfaces and the reflection due to material and surface treatment, both these artefacts require some pre-processing operations and an adequate set-up to perform image acquisition. These case studies represent a relevant application for the field of classic vehicle restoration, where C-RP could be a promising technique to support panel beaters and craftsmen during rebuilt operations of masks and bodywork spare parts of high-end historic cars.

Keywords 3D capturing · Close-range photogrammetry · 3D digital model · Geometric inspection · car body panel · Classic vehicle restoration

1 Introduction

3D acquisition techniques are widely used in many application fields with the aim of capturing and collecting all the features (shape, dimensions, textures, surface treatment) of an artefact or product. This acquisition is typically performed with equipment able to capture the physical specifications and transfer them in a digital form. There are many factors to consider when choosing the most suitable 3D acquisition technique, as the performance of the instrument adopted with respect to the resolution and precision required, but also the specificity of the object to be acquired, in terms of surface dimensions and characteristics [1]. Cost, time and skills of the operator are also influencing factors.

In the industrial sector, 3D capturing techniques are effectively used in multiple areas and with different purposes, from Reverse Engineering (RE) to monitoring, from metrology and inspection to digitizing and computer vision [2–4], due to the increasing performance of the adopted tools and technologies. In fact, due to their benefits in cost and time saving, 3D digital acquisition started to be essential tools to support the product design phases. Typical equipment adopted in the industrial and mechanical field are the active sensors, e.g., laser and structured-light 3D scanners, which guarantee a high level of detail and dimensional precision, thanks to their resolution. The widespread diffusion of 3D scanners is conversely limited by their high cost, which is not always affordable. Moreover, their use is not very easy, due to their complexity and the variety of models, with different functions and operating principles [5–7]. This is especially true for small-sized companies or craftsmen, due to the infrequent use of 3D scanners in everyday

The original online version of this article was revised: The corrected version of figure 1, caption and Image credits updated.

✉ Francesco Gherardini
francesco.gherardini@unimore.it

[1] Department of Engineering “Enzo Ferrari”, University of Modena and Reggio Emilia, Modena, Italy

applications / tasks, making equipment rental or outsourced services preferable.On the other hand, compared to other solutions, image-based modelling techniques [1] present cost-effectiveness, flexibility and efficient data acquisition as main advantages. Their ease-of-use, however, depends on the engineering know-how and the skills of the operators. In particular, a promising alternative to the use of 3D scanners is close-range photogrammetry (C-RP) [8–9], which thanks to a Structure-from-Motion (SfM) approach can extract corresponding image features from a series of overlapping photographs captured by a camera moving around the object. C-RP is widely applied in many fields, from archaeological and cultural heritage [10–12] to architecture [13–15], up to applications in medicine [16–18] and industry [19–21].

In the industrial fields, C-RP is mainly used for tool control and part inspection, structural and modal analysis, prototype and measurement control, assembly studies and production optimization [22–24]. In particular, the automotive industry shows an increasing demand of 3D reconstruction [25–26], where most of the C-RP applications lead to 3D reconstructions consistent with their specific goals. Since C-RP is able to capture a wide size range of artefacts, it can be adopted for vehicle body panels acquisition [22, 24, 26–27], for control and measuring tasks [22–23, 28–29], using metrology systems and optical coordinate measurement, for car safety testing and accident reconstructions [30]. Moreover, C-RP can carry out deformation measurements and modal analysis [3, 31–32] of free-form surfaces and Digital Image Correlation to obtain the mode shape of car body panels, as well as for aerodynamics and thermal simulations [27]. C-RP is also applied to achieve the virtual prototyping of automotive components [33], and the 3D surface measurement of a rear lamp housing of a vehicle using digital fringe projection system [34]. Moreover, the photogrammetric measurement and reconstruction of a full car model is presented in [27], with the aim of carrying out a thermal behaviour analysis, facing the problems related to the reflective surfaces and proposed solutions even if without quantitative validation of the accuracy of the acquisition.

Similarly to other optical 3D techniques, C-RP is sensitive to the presence of additional specific means (targets, adapters, etc.), whose presence has a positive impact on the accuracy of the reconstruction. If generally C-RP shows limitations in capturing mechanical features such as sharp edges and detailed geometries, using specific edge or borehole adapters, even those features can be measured. Again, C-RP can be advantageously applied to smoother shapes and surfaces, e.g., the vehicle bodywork and other aesthetical elements, if presenting sufficient texture or if targets are used.

The literature review highlights the suitability of C-RP to provide suitable 3D models for the industrial and automotive field, according to the VDI/VDE guidelines [35], which provide standardization and procedures for accuracy assessment of optical 3D measuring systems. Compared to C-RP, which requires adequate know-how and skills of the operator, the use of an industrial 3D scanner for close range applications can generally provide a reliable capture of point clouds, with a lower training threshold of the operator.

Therefore, this work aims to test and assess the use of C-RP to capture objects focusing on its strengths: the use of low-cost equipment such as a camera for amateur photographers (e.g., an ordinary compact digital camera) and free or affordable software, and the familiarity of most users with photography, requiring a limited additional effort in training and knowledge. This would spread the use of C-RP to automotive craftsmen and car restorers, who can benefit from the support of digital tools for the cost-effective creation of 3D virtual models. With this in mind, we would test this C-RP approach to capture car bodywork components, or other free-form artefacts, and generate their 3D models.

Considering the listed simplifications in the use of C-RP, we apply a systematic approach to assess its applicability to reach the expected goals. Firstly, the 3D acquisition of the car bodywork components is performed using more than one C-RP software, in order to achieve a more generalizable analysis, with lower dependency on (with respect to) the software functionalities. Secondly, the 3D model obtained using each C-RP software is compared to the one achieved by a 3D scanner, i.e. a state-of-the-art tool for the industrial sector; consequently, the C-RP models are also compared with each other.

The analysis is applied and assessed thanks to two different case studies belonging to the classic vehicle restoration field, namely a front lamp housing and a scaled front hood of classic Ferrari models. Typical problems related to the effective acquisition of this type of artefacts are the double curvature surface and the reflection due to the material and the surface finishing.

The paper is organized as follows. Section 2 presents the workflow for the assessment of the C-RP-based acquisition using low-cost camera and a simplified approach. In Sect. 3, the case studies are described and the workflow is applied. At the end of the paper, experimental results are analysed and discussed.

2 Method

This section introduces the general workflow of the C-RP approach, whose definition is useful to understand the software effects on the results. With this aim, C-RP based on compact digital camera photos is considered. The photogrammetric process for the 3D digital reconstruction of

physical objects is composed of three main phases, plus a final assessment phase: the pre-processing phase, the acquisition phase, the post-processing phase and the comparison and analysis of the results. These phases can be divided in the following steps:

(1) Evaluation of the original surface, in order to guarantee the best image quality.
    a) Ensure homogeneous light conditions around the object, avoiding shiny areas or reflections. Apply matting spray or polarising filter, if necessary.
    b) Place a scale bar and/or a reference coordinate system, with markers or calibrated control points, in the scene or around the object.
(2) Plan the set of photographs around the subject to provide high overlaps of the subject points, capturing the whole geometry. A rigid board is used for scaling and defining the reference coordinate system, with markers as target elements, which is accurately measured in laboratory. The reference coordinate system is fixed on the rigid board with the plane XY, considered horizontal, and the Z axis vertical.
(3) Image acquisition through the camera.
(4) Upload and import the photographs in the photogrammetric software.
(5) 3D model reconstruction through the software by setting image orientation and alignment, dense surface reconstruction and filtering. Further operations consist of:
    a) Cutting the scene surrounding the object (by manually deleting unnecessary points or using automatic masking procedures), except for the reference elements useful to align the models during the comparison phase.
    b) Model scaling using reference elements in the scene (e.g., the rigid board we used as a base for the components): the photogrammetric models can be scaled directly in the C-RP software as well as in a further software.
(6) Model comparison using reference models (i.e. 3D models acquired through alternative techniques and CAD models, if available) and analysis of the results. To compare the models, they need to be correctly aligned and then overlaid. In the comparison software (e.g., Geomagic Qualify X), the results are presented as graphical comparisons between the reference and the tested model, thanks to full colour deviation maps, multiple views including 2D and 3D dimensions and cross sections. Each single point of the models can be queried and sections following the geometrical features of the model can be used for detailed analysis.

In particular, the starting phase of surface assessment is crucial to obtain the best results from the 3D acquisition. The main limitations of C-RP are related to the artefact geometry (sharp edges, holes, undercuts, overall shape and dimensions) and surface finishing (textures, colours, surface treatment). Again, environmental factors (light exposition, reflective ambience properties, etc.) may negatively affected the whole process, so great care must be taken during the preparation phase. Researchers have studied the problem in several ways, such as Rosati et al. [36], who performed real-time defect detection on highly reflective curved surfaces. The detection of reflective surfaces is still a weak point for this technique, currently avoided through surface treatments, using matting sprays, markers or fringe projection. The proposed case studies are a challenging example of this acquisition issue due to their double curvature surfaces, surface treatments and materials.

The high dependence of the photogrammetric reconstruction on the quality and number of images, as well as the performance of the camera, requires to carefully plan the set of photographs, capturing the whole geometry of the object (i.e. through images taken all around the object at different heights).

A scaling operation is required since, unlike other 3D acquisition techniques, the objects acquired through photogrammetry have no absolute scale (i.e. the object size is not the real one). Depending on the software used, the introduction of the metric and the correct dimensions can be complex and could lead to scaling errors.

The described approach collects the best practises for the C-RP 3D reconstruction to choose the proper set-ups and tools based on the acquisition target as well as the surface features.

A large number of 3D acquisition and reconstruction software are available. Despite the differences in performance and price, the operating principle remains the same: after importing the photographs, the software reconstructs the geometry and the dense point cloud is processed. Then, a surface composed of polygons is reconstructed to obtain a mesh, whose vertices are the points of the cloud. After additional decimation, retopology and scaling operations, the model is ready to be imported and used in the CAD environment.

3 Results

The case studies developed in the present research work are bodywork components from two classic Ferrari models. In particular, a 1:5 scale model of front bonnet (hood) of a Ferrari 250 Testa Rossa from 1958 and a head lamp (light) housing of a Ferrari 275 GTB from 1964 are considered (Fig. 1).

The two artefacts consist of 1.5 mm aluminium sheets appropriately shaped by panel beaters. The geometries are characterized by a double curvature, with large curved panels without particular elements or geometric motifs (patterns, holes, knurls, etc.). In addition, the surface finishing of the polished aluminium surfaces has to be considered, especially for the lamp housing. The lack of patterns or reference elements and the reflection of the surface have to be considered as potential issues.

The 3D acquisition of these components through C-RP was performed using two different ordinary compact digital cameras (which are detailed in the following subsections). Two different software were applied: the free version of Autodesk ReCap Photo and the standard version Agisoft Metashape (chosen among the most used and affordable software). These software are both very effective, but they differ in cost and acquisition management: ReCap Photo (which replaces the software 123D Catch and ReMake) has a free version that can process a maximum number of 100 photos through a cloud-based system using default settings. However, ReCap Photo software has been used in many research works, showing its good overall qualities [7, 37]. On the other hand, the standard version of Metashape (the so-called "standard edition", with a permanent and affordable license)

a b

Fig. 1 Bodywork components proposed as case studies: a) a 1:5 scale model of front bonnet (top) of a Ferrari 250 Testa Rossa (bottom, photo credits: Prova MO, source: https://commons.wikimedia.org/wiki/File:1958_Ferrari_250_TR_0736TR_Front.jpg) and b) a head lamp housing (top) of a Ferrari 275 GTB (bottom, photo credits: RAVDesigns, source: https://commons.wikimedia.org/wiki/File:Ferrari275GTB-07241-LimeRock2015.jpg)

has no limits in the number of photos to be processed, it is more complete in terms of management and customisation of the geometric reconstruction, but the processing times are longer when setting a high level of accuracy and quality of reconstruction. The same set of photos were used to obtain comparable results and quantify the software performance. Moreover, to assess the C-RP as an alternative solution to 3D scanners, we used a structured light scanner to generate a reference model: the Zeiss Comet 6 8 M 3D Scanner with Blue LED structured light projection (Camera resolution: 8 Mpixel, (3296 × 2472); Max. resolution: 0.026 mm). Once the 3D models have been generated through C-RP and 3D scanning, the comparison was carried out using Geomagic Control X.

3.1 Ferrari 250 Testa Rossa engine bonnet

Firstly, the scale model of the Ferrari 250 Testa Rossa bonnet was considered.

(1) The main panel presents a slight curvature along both longitudinal and transverse directions. It is characterized by a vent for the engine air intake duct, placed in the central area of the bonnet: the vent is obtained by welding a curved panel and mounting a grille. The scale of the model is 1:5, with a final size of 352 × 310 × 53 mm. The artefact shows the typical surface finishing of the manual beating operation, leading to a matte and rough surface and not very reflective.

   a) To ensure the best acquisition, the artefact was placed on a rectangular board with circular markers and positioned in an open area to ensure a diffuse and natural light condition, avoiding reflections.
   b) Thanks to the surface finishing, neither markers nor matting spray were used on the artefact to simplify the set-up process.

(2) The set of photographs (Fig. 2a) were planned according to the geometry and the shape of the bonnet details. In order to provide high overlaps of the whole geometry, in particular to capture the double curvature surface and the shape of the air vent, photographs were taken around the entire artefact, at different angles (every 15–20°) and heights, maintaining a fixed distance with respect to the object.

(3) In the image acquisition phase, a compact digital camera Nikon P310 has been used, with 16.1 Mpixel CMOS sensor (sensor size: 1/2.3" ~ 6.16 mm x 4.62 mm, max. image resolution: 4608 × 3456, pixel size 1.34 µm, crop factor 5.62, focal length 4.3 ÷ 17.9 mm, 4.2 x optical zoom, maximum aperture f / 1.8 ÷ 4.9). Focal length

was set to minimal value during the entire shooting session for more stable results, with aperture f / 1.8, the exposure value equal to 0, exposure time: 1/1000 s, automatic ISO has been set, white balance has been blocked, flash has never been used, and manual focus has been enabled. 57 photos of the bonnet (JPG format) were taken.

(4) The set of photos was imported in both the software.

(5) The 3D models were generated respectively using Autodesk ReCap Photo (default setting) and Agisoft Metashape (Alignment accuracy: high; Dense point cloud generation quality: high, with mild depth filtering; Meshing quality: high). In Metashape, all the 57 images were aligned (with the results of camera calibration and image alignment as in Table 1). The generation of the 3D models (Fig. 2b) through C-RP required 2 h 10 min with ReCap Photo and 3 h 09 min with Metashape (processor i7-8850 H with 2.6 GHz CPU, NVIDIA Quadro 2000, 16 GB RAM). Then:

a) We cut the scene surrounding the object except for the board, where the bonnet was positioned, to simplify the model alignment during the comparison phase.

b) In Geomagic Control X, we scaled the models obtained from C-RP (Fig. 2d) using the board with markers. Then, they were correctly aligned and overlaid.

(6) The comparison between the models have been performed on the entire surfaces. However, to highlight the deviations along the main curvature of the bonnet, we generated five main sections: firstly, a cross plane normal to the longitudinal direction was placed in the middle of the bonnet (plane 0), then four additional cross planes were positioned at distance of -140, -70, 70, 140 mm with respect to plane 0. Three comparisons were performed: (A) the ReCap Photo model and the 3D scanned model (Fig. 3), (B) the Metashape model and the 3D scanned model (Fig. 4), (C) the ReCap Photo and Metashape models (Fig. 5).

A. In the first comparison between the ReCap Photo (Fig. 3a) and 3D scanner (Fig. 3b) models, the full colour deviation map (Fig. 3c) shows maximum positive deviation areas (yellow areas) between 0.5 and 0.8 mm, while the maximum negative deviation areas (blue areas) have values between −0.5 and −0.9 mm. These errors are located in restricted areas: on the outer edge of the air vent and, in particular, on the left surface of the vent itself, probably due to a reflection and / or an incorrect digitization on the sharp edge. The values resulting from this comparison are: average deviation: 0.091 mm, positive average deviation: 0.271 mm, negative average deviation: -0.160 mm and standard deviation: 0.552 mm. The main panel surface looks a bit 'spotty', probably due to its surface finishing. The cross sections of Fig. 3d show the reference model as continuous red lines and the tested model as single points, highlighting the areas with maximum deviation.

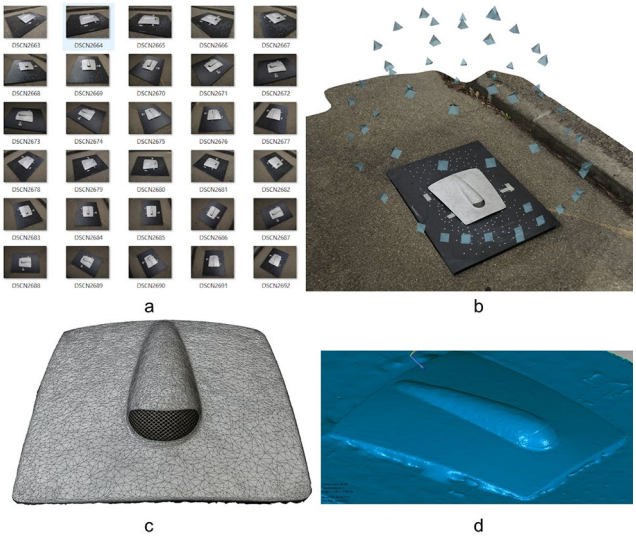

Fig. 2 The scale model of the Ferrari 250 Testa Rossa bonnet: (a) set of photos, (b) C-RP model, (c) meshed model, (d) final model (stl format)

B. In the second comparison between the Metashape (Fig. 4a) and 3D scanner (Fig. 4b) models, the full colour deviation map (Fig. 4c) shows maximum positive deviation areas (yellow areas) between 0.6 and 0.85 mm, while the maximum negative deviation areas (blue areas) present values between −0.6 and −0.85 mm. Differently to the previous comparison, the errors are located in different areas: on the outer edge of the bonnet, on the edge of the air vent and on the surface of the vent itself. The values resulting from this comparison are: average deviation: -0.013 mm, positive average deviation: 0.329 mm, negative average deviation: -0.321 mm and standard deviation: 0.739 mm. As in the previous case, the main panel surface looks 'spotty'. The cross sections of Fig. 4d highlight the areas with maximum deviation between the reference model (red lines) and the tested model (single points).

C. The final comparison between ReCap Photo (Fig. 5a) and Metashape (Fig. 5b) models shows a high similarity of the models, except for the areas in the edges and the air vent with higher positive and negative values, as observed also in the previous comparisons thanks to the full colour deviation map (Fig. 5c). The values resulting from this comparison are: average deviation:

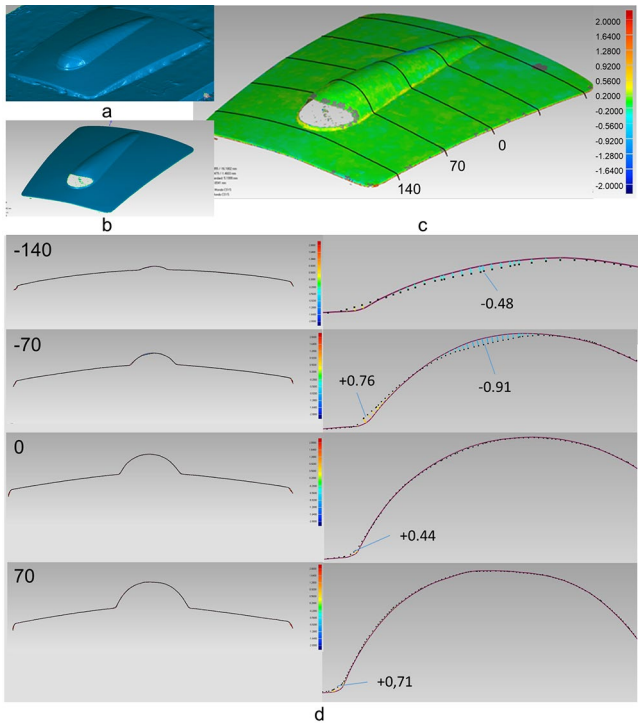

Fig. 3 Comparison A between (a) the ReCap Photo model and (b) the 3D scanned model; (c) full colour deviation map and cross sections on the compared models; (d) 2D views of significant sections (on the left) and deviation areas (on the right). The colour scale shown in c) is the same in all the figures

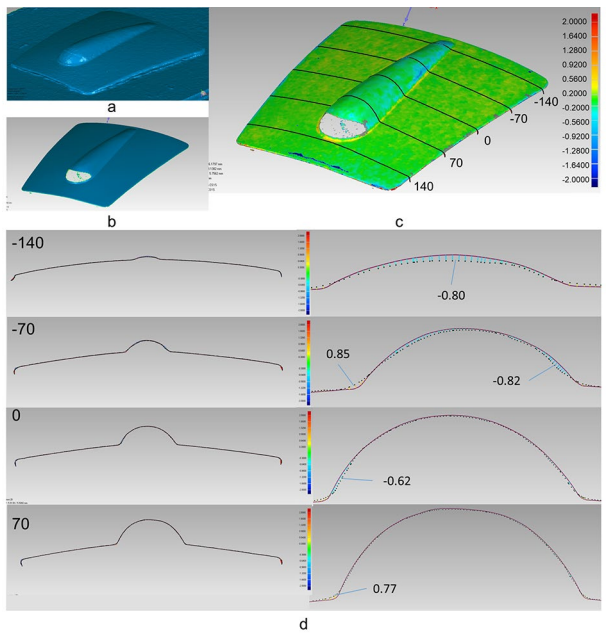

Fig. 4 Comparison B between (a) the Metashape model and (b) the 3D scanned model; (c) full colour deviation map and cross sections on the compared models; (d) 2D views of significant sections (on the left) and deviation areas (on the right). The colour scale shown in c) is the same in all the figures

-0.052 mm, positive average deviation: 0.153 mm, negative average deviation: -0.299 mm and standard deviation: 0.378 mm. The ReCap Photo model was set arbitrarily as the reference model and the Metashape model as the tested model (respectively shown as continuous red lines and as single points in the section views of Fig. 5d).

3.2 Ferrari 275 GTB front lamp housing

Even if the overall size is similar, the second case study presents geometric specificities.

1) The lamp housing has a strong curvature and a conical shape (Fig. 6a, top), due to the folding operation along a main axis of the aluminium sheet. Both sides of the lamp housing present a flanged edge: the inner one to position the lamp and fix the housing, and the outer one to align and join the entire housing to the car body. The folded shape of the component and the flanged edges affect the acquisition process. An additional issue is due to surface finishing: the polished surface is shiny and, except for the edges, highly reflective.

   a) To ensure the best acquisition, the artefact was placed on a rectangular rigid board with circular markers and positioned in an open area to ensure a homogeneous and adequate light condition. However, the surface presents reflections, in particular in the high curvature conical area of the housing.
   b) Due to the highly reflective surface, the application of a matting spray was necessary, paying attention to distribute it homogeneously and avoiding local stratifications. Since only the inner surface of the housing is visible when the vehicle is assembled, only this surface has been captured. In addition, due to the lack of references of the lamp housing surface (e.g. details, features, texture, etc.), geometric patterns were manually added on the conical surface (Fig. 6a, bottom).

2) The set of photographs were planned according to the different shape of the housing, considering its longitudinal extent. In order to provide high overlaps of the geometry, the photographs were taken at different angles (every 15–20°) and at different heights, with particular attention to capture the curved surface and the flanged edges, which can generate hidden areas.
3) In the acquisition of the lamp housing, a compact digital camera Canon Ixus 157 has been used, with 20 Mpixel CMOS sensor (sensor size: 1/2.3"~ 6.16 mm x 4.62

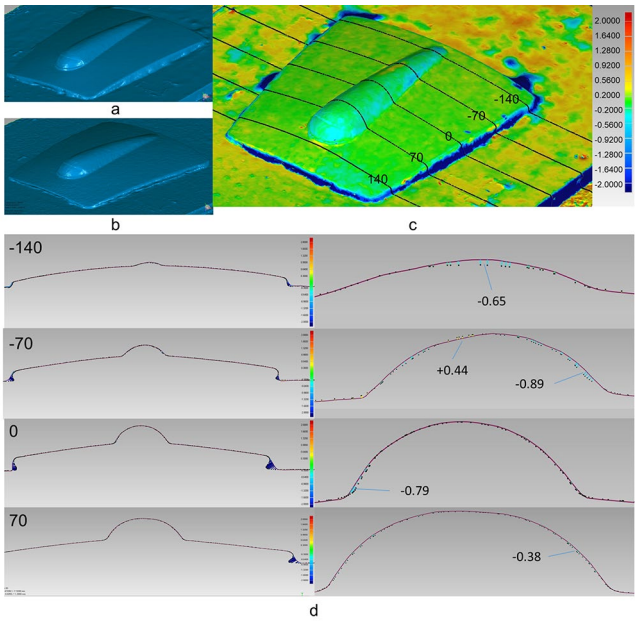

Fig. 5 Comparison C between the (a) ReCap Photo model and (b) Metashape model; (c) full colour deviation map and cross sections on the compared models; (d) 2D views of significant sections (on the left) and deviation areas (on the right). The colour scale shown in c) is the same in all the figures

Table 1 Results of camera calibration and adjusted alignment in Agisoft Metashape

Root Mean Square (RMS) reprojection error: 0.20 (0.60 pix)	Max. reprojection error: 0.61 (20.73 pix)
Principal point cx: 11.02 pix	Principal point cy: -22.59 pix
k1: -0.015828	k2: -0.017103
p1: -0.000295	p2: -0.001920
b1: 0	b2: 0

mm, max. image resolution: 5152 × 3864, pixel size 1.19 µm, crop factor 5.62, focal length 4.3 ÷ 43 mm, 10 x optical zoom, maximum aperture f / 3 ÷ 6.9). Focal length was set to minimal value during the entire shooting session for more stable results, with aperture f / 1.8, the exposure value was set equal to -2/3, exposure time: 1/200 s. automatic ISO has been set, white balance has been blocked, flash has never been used and autofocus has been enabled. 100 photos of the lamp housing (JPG format) were taken.

4) The set of photos was imported in both the software.
5) The 3D models were generated respectively using Autodesk ReCap Photo (default setting) and Agisoft Metashape (alignment accuracy: high; Dense point cloud generation quality: high, with mild depth filtering; Meshing quality: high). In Metashape, all the 100 photos were aligned (with the results of camera calibration and image alignment as in Table 2). The generation of the 3D meshed models (Fig. 6b, top) with both the software requires around 3 h with ReCap Photo and 5 h 30 min with Metashape.

   a) The scene surrounding the 3D models was cut except for the board, used during the model alignment.
   b) The models (Fig. 6b, top and bottom) were imported into Geomagic Control X, where the models obtained from C-RP have been scaled using the board as a reference. Then, they were aligned and overlaid.

6) The comparison between the models have been performed on the entire surfaces. In addition, to highlight the radial deviation of the surface, we generated seven cross sections, distributed along the height of the housing: starting from the inner flanged edge, the sections were set at a distance of 15, 50, 100, 150, 200, 250 and 300 mm. As for the bonnet model, three comparisons were performed between: (A) the ReCap Photo model and the 3D scanned model (Fig. 7), (B) the Metashape model and the 3D scanned model (Fig. 8), (C) the ReCap Photo and Metashape models (Fig. 9).

A. In the first comparison between the ReCap Photo (Fig. 7a) and 3D scanned (Fig. 7b) models, the full colour deviation map (Fig. 7c) shows maximum positive deviation areas (yellow areas) with values between 0.4 and 0.6 mm, while the values of the maximum negative deviation areas (blue areas) vary between − 0.5 and − 0.7 mm. These errors are mainly located in both the flanged areas, due to the sharp edges digitization, and in spotted inner areas. The cross sections of Fig. 7d show the reference model as continuous red lines and the tested model as single points, highlighting the areas with maximum deviation. The values resulting from this comparison are: average deviation: 0.035 mm, positive average deviation: 0.276 mm, negative average deviation: -0.301 mm and standard deviation: 0.469 mm.
B. In the second comparison between the Metashape (Fig. 8a) and 3D scanner (Fig. 8b) models, the full colour deviation map (Fig. 8c) shows that the upper part of the surface presents higher precision: most of the surface is within the ± 0.35 mm range. Conversely, in the lower part of the surface, where the curvature is higher and there are more sharp edges, the negative deviation (blue areas) increases, with values between − 0.3 and − 0.9 mm. These deviations are related to difficulties in the detection of the sharp edges and / or the light conditions. Furthermore, the maximum positive deviations (yellow areas) are limited in a few areas, with values

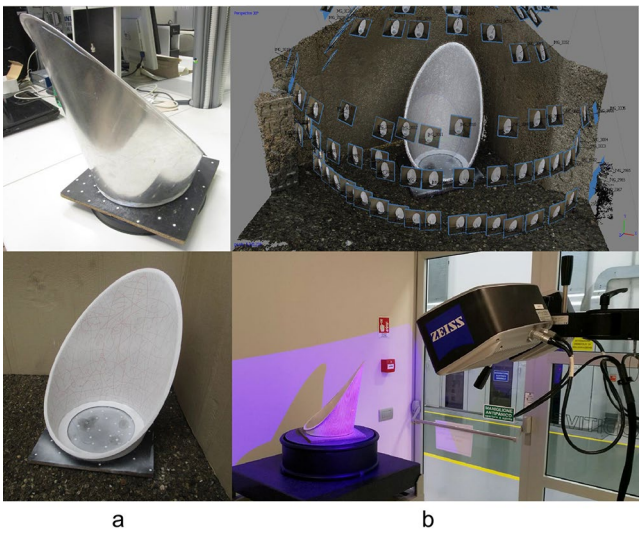

Fig. 6 The model of the Ferrari 275 GTB lamp housing: the lamp housing without (a, top) and with the matting spray (a, bottom); the C-RP model (b, top) and the 3D scanning phase (b, bottom)

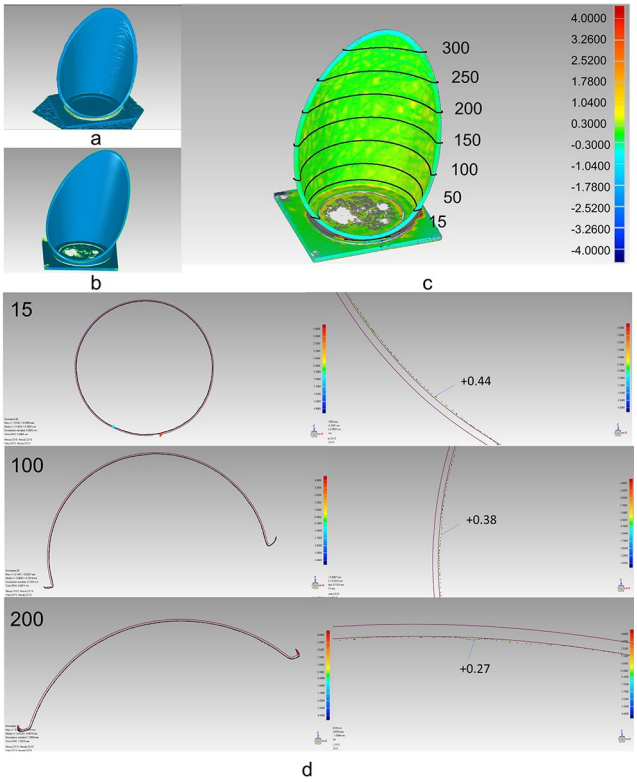

Fig. 7 Comparison A between (a) the ReCap Photo model and (b) the 3D scanned model; (c) full colour deviation map and cross sections on the compared models; (d) 2D views of significant sections (on the left) and deviation areas (on the right). The colour scale shown in c) is the same in all the figures

between + 0.3 and + 0.5 mm. Differently to the previous comparison, the outer flanged edge presents a poor quality irregular surface, probably due to light reflection. The cross sections of Fig. 8d highlight the areas with maximum deviation between the reference model (red lines) and the tested model (single points). The values resulting from this comparison are: average deviation: -0.038 mm, positive average deviation: 0.335 mm, negative average deviation: -0.348 mm and standard deviation: 0.747 mm.

C. The comparison between ReCap Photo (Fig. 9a) and Metashape (Fig. 9b) models returns the full colour deviation map of Fig. 9c. The ReCap Photo model presents an irregular surface due to homogeneously distributed "spots", which show similar values of deviation in most of the housing surface. Conversely, the Metashape model has a higher precision in the upper area, is more regular and the inner surface looks less 'spotty', but the flanged edges show higher deviations and the mesh is less smooth. Both these models share a common trend due to the geometric patterns of the conical surface, which lead to small deviations from the nominal except in some restricted areas (Fig. 9d). In the comparison, the ReCap Photo model was set arbitrarily as the reference model and the Metashape model as the tested model (respectively shown as continuous red lines and as single points in the section views of Fig. 9d). The values resulting from this comparison are: average deviation: -0.024 mm, positive average deviation: 0.210 mm, negative average deviation: -0.429 mm and standard deviation: 0.697 mm.

4 Discussion and conclusion

This work presents the results of the application of a low-cost and simplified approach to C-RP to car bodywork components or similar free-form artefacts, to generate 3D models as a support for vehicle restoration. To make a more generalizable analysis, with lower dependency on the software functionalities, two commercial and widely used software, i.e. Autodesk ReCap Photo and Agisoft Metashape, are applied using the same set of photos. In order to assess a quantitative analysis, the method focuses on the benchmarking between the C-RP models and a reference model obtained by a 3D scanner, which is acknowledged as a state-of-the-art tool for the industrial field. The case studies show the performance of the simplified C-RP approach in different conditions, thanks to their specificities: the slight curvature and wrought surface of the bonnet with respect to the high-curvature and shiny head lamp housing. Therefore, different pre-processing operations are needed to perform the

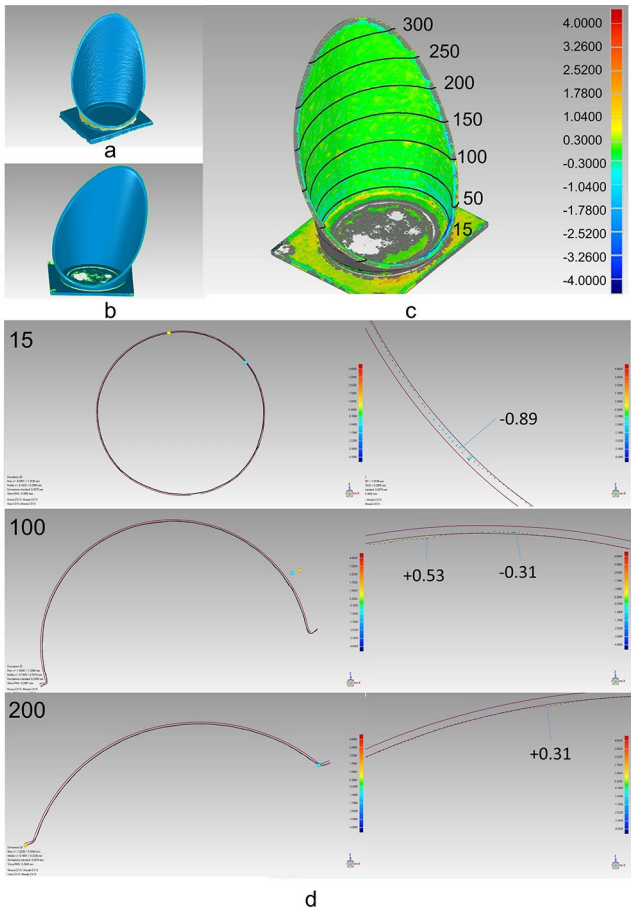

Fig. 8 Comparison B between (a) the Metashape model and (b) the 3D scanned model; full colour deviation map and cross sections on the compared models; d) 2D views of significant sections (on the left) and deviation areas (on the right). The colour scale shown in (c) is the same in all the figures

acquisition. Despite the noise introduced with the geometric patterns for the head lamp housing and the related spotted surfaces, both the automotive artefacts are fully acquired.

The results show that the average deviations from the reference model (i.e. the 3D scanned model), within the range of ±0.3 mm, are acceptable when compared to the variation limits of the handcrafted sheet metal working process in car restoration (the typical range is ± 1 mm). Even the maximum deviations are within this acceptable range: They are located in limited areas, such as boundaries, with sharp edges or small radii of curvature (abrupt changes in curvature), or as noise localized on homogeneous areas. Therefore, they are easily identifiable as a potential error and manually corrected.

The following specific remarks can be summed up:

- The overall behaviour of the two C-RP software is similar in the reconstruction of the two case studies, although their models slightly differ in some areas. Other differences are registered mainly in the processing time and functioning procedure.
- Some minor reconstruction defects or lacks of details are present in the sharp edges (e.g., in the lamp housing) or in the smallest changes of curvature (in both models). However, these deviations are acceptable with respect to the field of application.
- A careful setting is required during the acquisition phase, even if this does not increase the overall complexity of the procedure and the affordability of the requested equipment. In this way, even small-sized companies and craftsmen will be able to generate 3D models based on photographs taken with affordable cameras and low-cost software, ensuring consistency with the original car shape.

In conclusion, the 3D acquisition based on C-RP and the use of inexpensive cameras have proven to be practical here and suitable to be applied to a specific automotive field as the classic vehicle restoration, whose desired accuracy is in the range of 1 mm. In this way, C-RP may be considered as an affordable alternative to 3D scanning.

Further investigations are planned for the future, addressing some improvements with respect to the tools implemented and the areas of application.

In the first case, the use of better cameras is foreseen, identifying the trade-off between affordable equipment and the expected quality. Even if more expensive, a professional camera could improve the acquisition accuracy, proving to be more suitable for the specific application field. Moreover, additional investigations are foreseen by testing further SfM software with the same data.

In the second case, the digitization of the entire bodywork of still existing historic cars will be developed, following the same approach, with the aim of preserving their original shape, similar to the use of metal or wooden models (the so called “masks”) made in the past. Nowadays, the same goal can be achieved through 3D digital “masks”, which can be further used to develop physical tools, on which panel beaters will model and check the sheet metal to create also bodywork spare parts.

Acknowledgements The authors acknowledge the restoration shops Bacchelli & Villa (Bastiglia (Modena), Italy) and Brandoli Egidio (Montale Rangone (Modena), Italy) for providing the bodywork spare parts used as case studies.

Declarations

Image credits All images are by the authors, unless the two pictures at the bottom of Figure 1: the Ferrari 250 Testa Rossa (Fig. 1a, bottom), photo credits: Prova MO, licensed under the Creative Commons Attribution-Share Alike 4.0 International, source: https://commons.wikimedia.org/wiki/File:1958_Ferrari_250_TR_0736TR_Front.jpg,

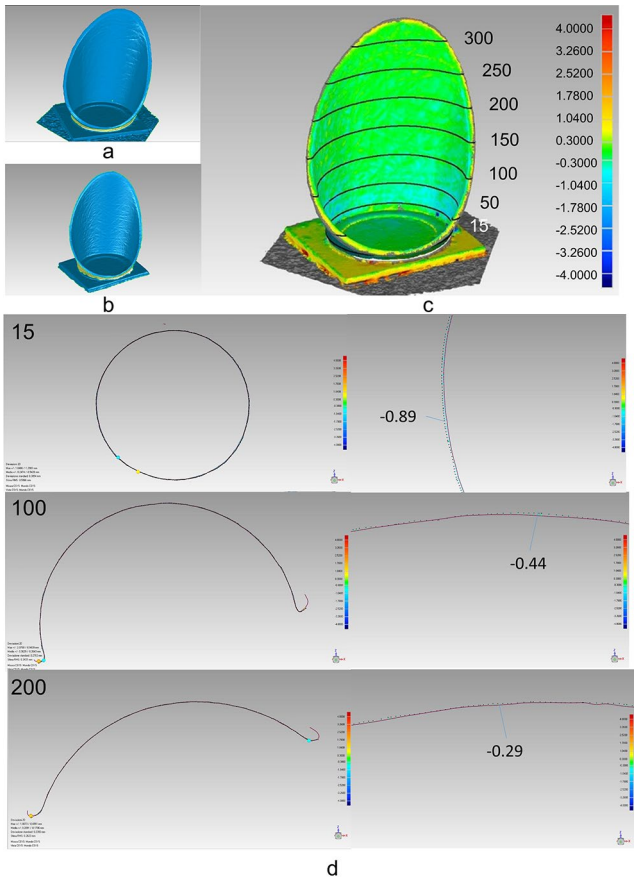

Fig. 9 Comparison C between the (a) ReCap Photo model and (b) Metashape model; (c) full colour deviation map and cross sections on the compared models; (d) 2D views of significant sections (on the left) and deviation areas (on the right). The colour scale shown in c) is the same in all the figures

Table 2 Results of camera calibration and adjusted alignment in Agisoft Metashape

Root Mean Square (RMS) reprojection error: 0.19 (0.82 pix)	Max. reprojection error: 0.60 (23.85 pix)
Principal point cx: 29.70 pix	Principal point cy: 61.46 pix
k1: -0.025566	k2: 0.002411
p1: 0.003395	p2: 0.003954
b1: 0.717829	b2: 0.746212

and the Ferrari 275 GTB (Fig. 1b, bottom), photo credits: RAVDesigns, licensed under the Creative Commons Attribution-Share Alike 2.0 Generic, source: https://commons.wikimedia.org/wiki/File:Ferrari275GTB-07241-LimeRock2015.jpg

Authors' declaration The authors declare no competing financial interest nor conflict of interest.

References

1. Guidi, G., Remondino, F.: 3D Modelling from real data. In: Modeling and Simulation in Engineering, edited by A. Catalin, 69–102. London: IntechOpen: (2012) doi: https://doi.org/10.5772/30323
2. Sedlak, J., Polzer, A., Chladil, J., Slany, M., Jaros, A.: Reverse engineering method used for Inspection of Stirrer's Gear box cabinet prototype. MM Sci. J. I (November), 1877–1882 (2017). doi:https://doi.org/10.17973/MMSJ.2017_11_201719
3. Godding, R., Luhmann, T., Wendt, A.: 4D Surface matching for high-speed stereo sequences. Proceedings of the ISPRS Symposium Commission V 2 (2) (September). Dresden: (2006)
4. Raffaeli, R., Mengoni, M., Germani, M., Mandorli, F.: Off-line view planning for the inspection of mechanical parts. Int. J. Interact. Des. Manuf. **7**, 1–12 (2013). doi:https://doi.org/10.1007/s12008-012-0160-1
5. Blais, F.: Review of 20 years of range sensor development. J. Electron. Imaging. **13**(1), 231–243 (2004). doi:https://doi.org/10.1117/1.1631921
6. Barsanti, S.G., Remondino, F., Visintini, D.: Photogrammetry and laser scanning for archaeological site 3D modeling - some critical issues. In: Proceedings of the 2nd Workshop on The New Technologies for Aquileia (NTA-2012), Aquileia, Italy, 25 June, 2012. B1-B10 (2012)
7. Parras, D., Cavas-Martínez, F., Nieto, J., Cañavate, F.J.F., Fernández-Pacheco, D.G.: Reconstruction by low cost software based on photogrammetry as a reverse engineering process. Lecture Notes in Computer Science (10909), pp. 145–154. Cham: Springer International Publishing (2018). doi:https://doi.org/10.1007/978-3-319-91581-4_11
8. Luhmann, T., Robson, S., Kyle, S., Böhm, J.: Close-range photogrammetry and 3D imaging. De Gruyter, Berlin (2019). doi:https://doi.org/10.1515/9783110607253
9. Cooper, M.A.R., Robson, S. Theory of close range photogrammetry, in: Close Range Photogrammetry and Machine Vision, Whittles Publishing, Roseleigh House, Latheronwheel, Caithness, KW5 6DW, Scotland, UK, 2000, pp. 9–50
10. Haukaas, C., Hodgetts, L.M.: The Untapped Potential of Low-Cost Photogrammetry in Community-Based Archaeology: A Case Study From Banks Island, Arctic Canada. J. Community Archaeol. Herit. **3**(1), 40–56 (2016). doi:https://doi.org/10.1080/20518196.2015.1123884
11. Gherardini, F., Santachiara, M., Leali, F.: 3D virtual reconstruction and augmented reality visualization of damaged stone sculptures. IOP Conference Series: Materials Science and Engineering 364(1), 012018. Florence: IOP Publishing Ltd: (2018). doi: https://doi.org/10.1088/1757-899X/364/1/012018
12. Ramm, R., Heinze, M., Kühmstedt, P., Christoph, A., Heist, S., Notni, G.: Portable solution for high-resolution 3D and color texture on-site digitization of cultural heritage objects. J. Cult. Herit. **53**, 165–175 (2022). doi:https://doi.org/10.1016/j.culher.2021.11.006
13. De Luca, L., Driscu, T., Peyrols, E., Labrosse, D., Berthelot, M.: A complete methodology for the virtual assembling of dismounted historic buildings. Int. J. Interact. Des. Manuf. **8**, 265–276 (2014). doi:https://doi.org/10.1007/s12008-014-0224-5
14. D'Ayala, D., Smars, P.: Architectural and structural modelling for the conservation of cathedrals. J. Architectural Conserv. **9**(3), 51–72 (2003). doi:https://doi.org/10.1080/13556207.2003.10785351
15. Mikoláš, M., Jadviščok, P., Molčák, V.: Application of terrestrial photogrammetry to the creation of a 3D model of the Saint Hedwig Chapel in the Kaňovice. Geodesy and Cartography. **40**(1), 8–13 (2014). doi:https://doi.org/10.3846/20296991.2014.906923

16. Grazioso, S., Selvaggio, M., Di Gironimo, G.: Design and development of a novel body scanning system for healthcare applications. Int. J. Interact. Des. Manuf. **12**, 611–620 (2018). doi:https://doi.org/10.1007/s12008-017-0425-9
17. Galantucci, L.M., Percoco, G., Maso, D.: U.: Coded targets and hybrid grids for photogrammetric 3D digitisation of human faces. Virtual and Physical Prototyping. **3**(3), 167–176 (2008). doi:https://doi.org/10.1080/17452750802259603
18. Sansoni, G., Cavagnini, G., Docchio, F., Gastaldi, G.: Virtual and physical prototyping by means of a 3D optical digitizer: Application to facial prosthetic reconstruction. Virtual and Physical Prototyping. **4**(4), 217–226 (2009). doi:https://doi.org/10.1080/17452750903236658
19. Hunt, R.A.: Photogrammetry in industrial measurement. In: Williams, D.C. (ed.) Optical Methods in Engineering Metrology. Engineering Aspects of Lasers Series. Springer, Dordrecht (1993). doi:https://doi.org/10.1007/978-94-011-1564-3_4
20. Mendikute, A., Yagüe-Fabra, J.A., Zatarain, M., Bertelsen, Á, Leizea, I.: Self-Calibrated In-Process Photogrammetry for Large Raw Part Measurement and Alignment before Machining. Sensors. **17**, 2066 (2017). doi:https://doi.org/10.3390/s17092066
21. Percoco, G., Sánchez Salmerón, A.J.: 3D image based modelling for inspection of objects with micro-features, using inaccurate calibration patterns: an experimental contribution. Int. J. Interact. Des. Manuf. **11**, 415–425 (2017). doi:https://doi.org/10.1007/s12008-016-0342-3
22. Blagojević, M., Rakić, D., Topalović, M., Živković, M.: Optical coordinate measurements of parts and assemblies in automotive industry. Tech. Gaz. **23**(5), 1541–1546 (2016). doi:https://doi.org/10.17559/TV-20130918160442
23. Srivastava, V., Baqersad, J.: A multi-view optical technique to extract the operating deflection shapes of a full vehicle using digital image correlation. Thin-Walled Struct. **145**(December), 106426 (2019). doi:https://doi.org/10.1016/j.tws.2019.106426
24. Luhmann, T.: Close range photogrammetry for industrial applications. ISPRS J. Photogrammetry Remote Sens. **65**(6), 558–569 (2010). doi:https://doi.org/10.1016/j.isprsjprs.2010.06.003
25. Sansoni, G., Docchio, F.: In-field performance of an optical digitizer for the reverse engineering of free-form surfaces. Int. J. Adv. Manuf. Technol. **26**(11–12), 1353–1361 (2005). doi:https://doi.org/10.1007/s00170-004-2122-7
26. Parmehr, E.G., Azizi, A.: A Comparative Evaluation of the Potential of Close Range Photogrammetric Technique for the 3D Measurement of the Body of a Nissan Patrol car. Proceedings of the ISPRS XXXV Istanbul congress, Commission V, WG VI/1. Istanbul: (2004)
27. Thomas, M.A., Hassan, M.F., Salim, W.S.I., Azmir, S., Osman, H.M., Jalal, M.A.: Reconstruction of 3D Models in Automotive Engineering Applications Using Close-Range Photogrammetry Approach. J. Adv. Res. Fluid Mech. Therm. Sci. **61**(2), 220–232 (2019)
28. Mostofi, N., Samadzadegan, F., Roohy, S., Nozari, M.: Using vision metrology system for quality control in automotive industries. International Archives of the Photogrammetry, Remote Sensing and Spatial Information Sciences. Melbourne, Australia, 25 August 2012. 39, 33–37 (2012). doi: https://doi.org/10.5194/isprsarchives-XXXIX-B5-33-2012
29. Srivastava, V., Baqersad, J.: An optical-based technique to obtain operating deflection shapes of structures with complex geometries. Mech. Syst. Signal Process. **128**(March), 69–81 (2019). doi:https://doi.org/10.1016/j.ymssp.2019.03.021
30. Han, I., Kang, H.: Three-dimensional crush scanning methods for reconstruction of vehicle collision accidents. Int. J. Autom. Technol. **17**(1), 91–98 (2016). doi:https://doi.org/10.1007/s12239-016-0008-y
31. Patil, K., Srivastava, V., Baqersad, J.: A multi-view optical technique to obtain mode shapes of structures. Measurement. **122**, 358–367 (2018). doi:https://doi.org/10.1016/j.measurement.2018.02.059
32. Di Paola, F., Ingrassia, T., Lo Brutto, M., Mancuso, A.: A reverse engineering approach to measure the deformations of a sailing yacht. In: Eynard, B., Nigrelli, V., Oliveri, S., Peris-Fajarnes, G., Rizzuti, S. (eds.) Advances on Mechanics, Design Engineering and Manufacturing. Lecture Notes in Mechanical Engineering. Springer, Cham (2017). doi:https://doi.org/10.1007/978-3-319-45781-9_56
33. Renno, F., Terzo, M.: Close-range photogrammetry approach for the virtual prototyping of an automotive magnetorheological semi-active differential. Eng. Lett. **23**(3), 163–172 (2015)
34. Liu, C.Y., Wang, C.Y., Teng, L.W.: High-speed 3D surface measurement of rear lamp housing by automatic digital fringe projection system. Proceedings of Optical Technology and Measurement for Industrial Applications Conference 26 April, 2019. Yokohama, Article number OPTM-2-04 (2019)
35. VDI/VDE 2634: Optical 3D measuring systems. VDI/VDE guide line, Part 1–3, Beuth, Berlin
36. Rosati, G., Boschetti, G., Biondi, A., Rossi, A.: Real-time defect detection on highly reflective curved surfaces. Opt. Lasers Eng. **47**(3–4), 379–384 (2009). doi:https://doi.org/10.1016/j.optlaseng.2008.03.010
37. Santagati, C., Inzerillo, L., Di Paola, F.: Image-based modeling techniques for architectural heritage 3D digitalization: Limits and potentialities. International Archives of the Photogrammetry, Remote Sensing and Spatial Information Sciences -. ISPRS Archives. **40**(5W2), 555–560 (2013)